JOURNAL OF combinatorial CHEMISTRY

Article

Design of Combinatorial Shadow Masks for Complete Ternary-Phase Diagramming of Solid State Materials

R. Takahashi, H. Kubota, M. Murakami, Y. Yamamoto, Y. Matsumoto, and H. Koinuma

J. Comb. Chem., **2004**, 6 (1), 50-53• DOI: 10.1021/cc030038i • Publication Date (Web): 13 November 2003

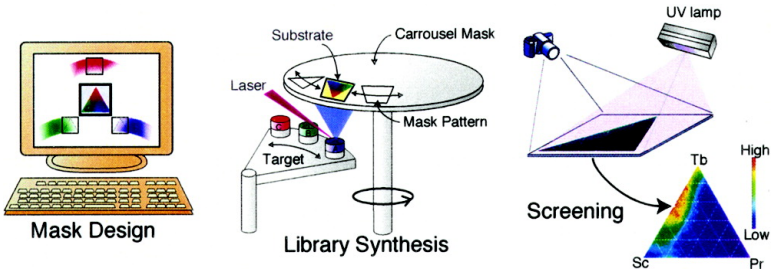

More About This Article

Additional resources and features associated with this article are available within the HTML version:

- Supporting Information
- Links to the 1 articles that cite this article, as of the time of this article download
- Access to high resolution figures
- Links to articles and content related to this article
- Copyright permission to reproduce figures and/or text from this article

View the Full Text HTML

Journal of Combinatorial Chemistry is published by the American Chemical Society.
1155 Sixteenth Street N.W., Washington, DC 20036

Design of Combinatorial Shadow Masks for Complete Ternary-Phase Diagramming of Solid State Materials

R. Takahashi,*[,†] H. Kubota,[†] M. Murakami,[†] Y. Yamamoto,[‡] Y. Matsumoto,[§] and H. Koinuma[†,‡,⊥]

Materials and Structures Laboratory, Tokyo Institute of Technology, 4259 Nagatsuda-tyo, Midori-ku, Yokohama 226-8502, Japan, National Institute of Material Science, 1-1 Namiki, Tsukuba, Ibaragi, Japan, Frontier Collaborative Research Center, Tokyo Institute of Technology, Yokohama 226-8503, Japan, and CREST, Japan Science and Technology Corporation, Japan

Received April 8, 2003

We report on a novel mask design for the combinatorial synthesis of a ternary composition spreads library, which allows such libraries to be deposited through a series of simple masks on a rotatable mount. This eliminates the use of complicated actuation of a heated substrate. In our configuration, this design leads to a standard linear phase diagram by varying the growth rate of each constituent nearly linearly from 0 to 100% at a triangular area on the substrate. Film growth occurs as a series of cycles in which one molecular layer of the material is deposited over the entire area of the spread by a synchronization of the mask movement, target exchange, and laser pulses. The technique has been applied to the synthesis of photoluminescent $TbCa_4O(BO_3)_3-ScCa_4O(BO_3)_3-PrCa_4O(BO_3)_3$, demonstrating its value for the mapping of direct relationship between composition and the light-emitting property.

Introduction

Various kinds of high-throughput thin-film synthesis techniques coupled with rapid characterization tools have been developed for exploring new compositions as well as for optimizing process parameters of materials.[1,2] Methods to prepare different types of combinatorial thin-film libraries include discrete sequentially masked depositions[3], composition spread co-deposition,[4] and composition-gradient molecular layer epitaxy.[5] These techniques have resulted in the discovery of many exciting new materials, such as Co-doped TiO_2 transparent magnets[6] and in the quick optimization of epitaxial thin film growth conditions.[7]

The continuous composition spread method using the co-deposition technique can be traced back to the report by N. C. Miller in 1967.[8] Subsequent reports came from Hanak's,[9] Koinuma's,[10] and other groups. Recently, van Dover's group investigated the dielectric properties of various ternary oxide systems, including $ZrO_x-SnO_y-TiO_z$.[4] Co-deposition is a simple process, but the distribution of the composition on a substrate cannot be directly controlled and must be determined independently by such an analytical technique as electron probe microanalysis (EPMA).[2,4] Another drawback of this method is the difficulty in covering the entire phase diagrams, because of the inevitable intermixing of chemical species evaporated from different sources. Formation of ternary composition spreads with predetermined composition distribution has been achieved by controlling the film deposition time or thickness at each position on the substrate with the aid of physical shadow mask movement and substrate rotation[11−13]. Nevertheless, this method still contains the weak point that the restless substrate rotation in the above combinatorial process is quite time-consuming and tends to cause mechanical troubles.

In this paper, we report on the computer-aided design of a new masking scheme (pattern and movement) for vapor deposition (molecular beam epitaxy, sputtering, pulsed laser deposition, etc.) of spatially addressable ternary composition spreads, as illustrated in Figure 1a. The main advantage of this deposition method in Figure 1b is its ability to create ternary-phase diagrams without substrate rotation and in the direct correlation between the library location (address) and composition, as in typical ternary-phase diagrams. A successful implementation of this method is reported for phosphors of $TbCa_4O(BO_3)_3$, $ScCa_4O(BO_3)_3$, and $PrCa_4O(BO_3)_3$ ternary system. The spreads are screened with high-throughput characterization methods, as illustrated in Figure 1c.

Equipment

Ternary composition spread libraries were synthesized by the combinatorial laser molecular-beam epitaxy (CLMBE), as illustrated in Figure 1b. In the CLMBE, molecular layers are deposited from several kinds of solid sources through a series of physical shadow masks placed on a heated substrate, and the deposited materials are crystallized in as-grown states.

The ternary composition spread is shaped into a 15-mm-side triangle by repeating the superposition of three different

* To whom correspondence should be addressed; E-mail: takahashi@oxide.msl.titech.ac.jp.
† Materials and Structures Laboratory, Tokyo Institute of Technology.
‡ National Institute of Material Science.
§ Frontier Collaborative Research Center, Tokyo Institute of Technology.
⊥ CREST.

10.1021/cc030038i CCC: $27.50
Published on Web 11/13/2003

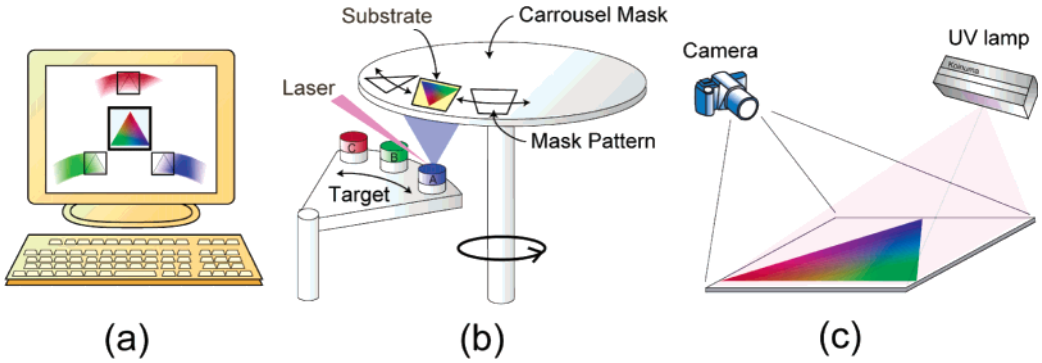

Figure 1. Schematic of experimental steps: (a) the computer-aided design of the shadow mask, (b) the synthesis of a composition spread, and (c) the rapid screening.

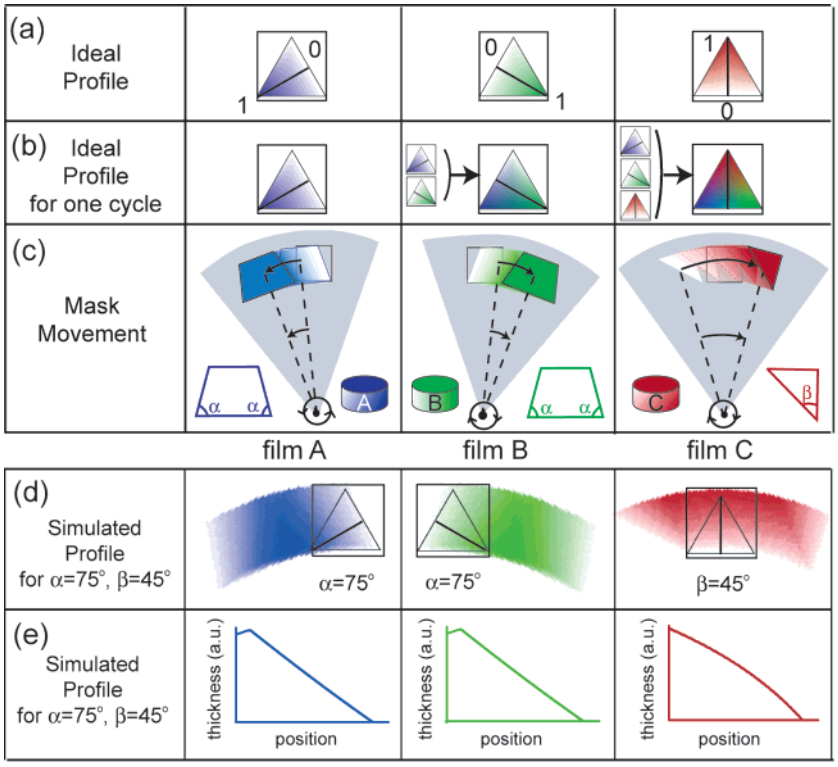

Figure 2. (a, b) Ideal deposition profile for each film to form a ternary-phase diagram. (c) Movement of the combinatorial masks on the carrousel holder. (d) Simulation mapping for $\alpha = 75°$ and $\beta = 45°$ (e) Simulation cross-sectional profile along the line in (d). A good linear thickness gradient was successfully achieved.

films of its thickness in a linear gradient along the three axes, separated by 120° rotations, as illustrated in Figure 2a,b. The total thickness of the three gradient films in a deposition cycle is made constant at one unit cell (0.8 nm). The elemental diffusion length should exceed the vertical film thickness of each deposition cycle on a heated substrate, whereas it should be short enough to give composition spread horizontally.

Figure 2c shows the shapes and movements of the shadow mask on a rotating holder (radius: 60 mm) in the CLMBE. To create film thickness gradients along the three axes separated by 120° rotations, we employed two shapes (trapezoid and triangle) of opening and optimized the angles α and β to make ternary-phase diagrams. For the simulation of film thicknesses at various positions on a substrate, the following functions are defined by eqs 1 and 2 for representing the film deposition "1" or not "0" and the film thickness at a spot (x, y) on the substrate, respectively.

$$\Delta\mathrm{Film}(x, y, \theta) = \begin{Bmatrix} 1{:}(x, y) \in \mathrm{mask}(\theta, \alpha, \beta) \\ 0{:}(x, y) \in \mathrm{mask}(\theta, \alpha, \beta) \end{Bmatrix} \quad (1)$$

$$\mathrm{thick}(x, y) = \sum_{n} \Delta\mathrm{film}(x, y, n\Delta\theta) \quad (2)$$

Here, θ is the rotation angle of the mask and $\Delta\theta$ is the rotation angle unit for calculating thick (x, y). The parameters α and β are characteristic of the mask shape as defined in Figure 2c. The total mask rotation angles are 20° for the trapezoid mask and 40° for the triangle mask, respectively. The mapping images of the thick (x, y) for $\alpha = 75°$ and $\beta = 45°$, and $\Delta\theta = 1°$ are depicted in Figure 2d. Figure 2e shows the cross-sectional profile along the line in the Figure 2d. The deposition profile for each film is almost identical to the ideal profile shown in Figure 2a. The average error in

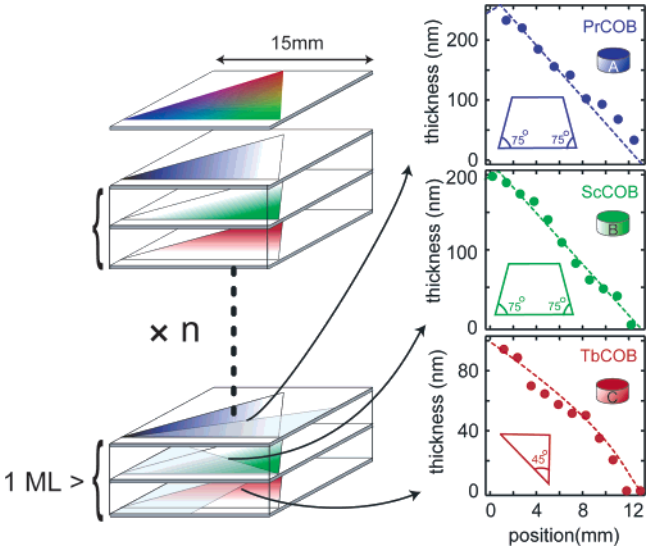

Figure 3. Thickness gradients of PrCOB (a), ScCOB (b), and TbCOB (c) films synthesized by repeating the deposition of each one of the films under the piston motion of shadow mask. The dotted line shows the simulation result in Figure 2e. The experimental thickness gradients are quite consistent with the simulation; a good linear thickness gradient was successfully achieved.

the composition is <5%, except for the near-edge region. On the basis of this result, we can produce a ternary-phase diagram or a composition spread library by repeating the deposition cycles of films A, B, and C under the conditions of forming each film where each thickness gradient across a triangle is from 0 to 0.8 nm. This condition can be satisfied easily by controlling the moving rates of the masks.

Experimental Section

The simulation was experimentally verified in the formation of a ternary composition spread of RCOB, where R and COB represent Tb, Sc, or Pr and $Ca_4O(BO_3)_3$, respectively. GdCOB and YCOB are known as nonlinear optical materials with transmittance in the range of 210−2600 nm, a high damage threshold, and a high chemical stability.[14] Tb atoms at the R site are known to induce luminescence of green light (542 nm) as a result of the $^5D_4 \rightarrow {}^7F_5$ transition under the irradiation of an ultraviolet source. To synthesize the ternary-phase diagram of $Tb_{1-x-y}Sc_xPr_yCa_4O(BO_3)_3$, TbCOB, ScCOB, and PrCOB films were deposited according to the procedure depicted in Figure 2. The oxygen pressure and substrate temperature were fixed to be 1×10^{-6} Torr and 800 °C, respectively.[15] TbCOB, ScCOB, and PrCOB ceramic targets were ablated by KrF eximer laser pulses (248 nm, 3J/cm^2, 10 Hz).

The deposition rates of components TbCOB, PrCOB, and ScCOB films were determined in advance by repeating the deposition of each one of the films under the piston motion of a shadow mask. The thickness gradients of films thus prepared were evaluated by the Stylus method (Sloan DEKTAK^{3}ST). As shown in Figure 3a−c, the thickness gradient of each film was quite consistent with that from the simulation (dotted line); a good linear thickness gradient was successfully achieved. A ternary composition spread film of $Tb_{1-x-y}Sc_xPr_yCa_4O(BO_3)_3$ (300 nm) was then synthesized on Al_2O_3(0001) and YCOB(100) substrates used for evaluating the film composition and growing epitaxial thin films, respectively. The film thickness of a deposition cycle was kept constant at one unit cell (0.8 nm thick) in the whole area by synchronizing the mask movement, target exchange, and laser pulses. This cycle was repeated 375 times in 20 h in order to obtain the designed thickness of 300 nm (= 0.8 × 375 nm). The linear change in composition as a function of position in the $Tb_{1-x-y}Sc_xPr_yCa_4O(BO_3)_3$ spread film on the Al_2O_3(0001) substrate was verified with EPMA, and the absence of impurity phases was confirmed by X-ray diffraction spectra of the film on the YCOB substrate.

The photoluminescence (PL) property of the spread film was investigated by taking a color photograph of the chip under excitation with an ultraviolet (254-nm) lamp (Figure 4a). The intensity of white light emission is shown in Figure 4b. A high-intensity light-emitting region was clearly observed in the intensity map. The $Tb_{0.6}Sc_{0.4}Ca_4O(BO_3)_3$ region had the brightest emission, and there was no positive effect of Pr. A similar PL intensity dependence in the composition was confirmed in the PL spectra of $^5D_4 \rightarrow {}^7F_5$ emission (542 nm) excited with a frequency-doubled Ar laser (488 nm). Details and discussions will be reported elsewhere.

Conclusion

We have designed a new mask system for synthesis of spatially addressable ternary-phase diagrams by various thin film synthesis processes, such as pulsed laser deposition. The

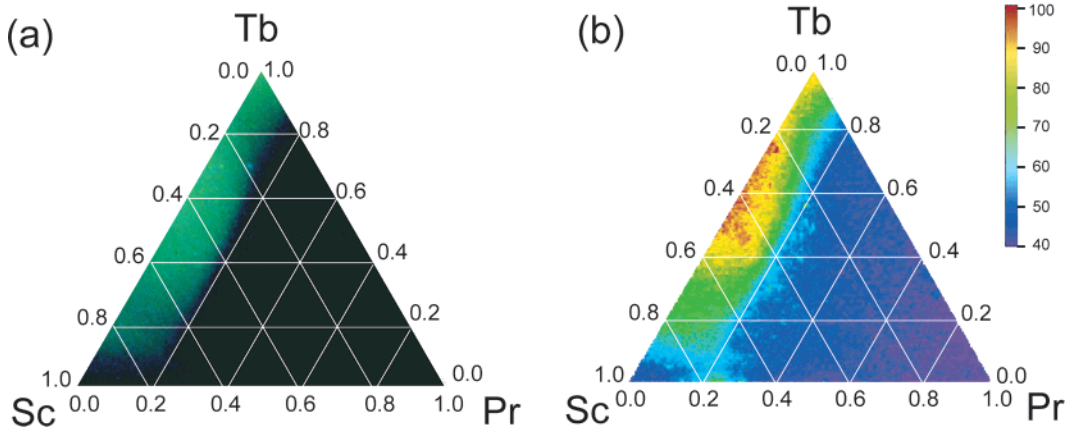

Figure 4. (a) Color photograph of the $Tb_{1-x-y}Sc_xPr_yCa_4O(BO_3)_3$ library under ultraviolet (254 nm) excitation. (b) Intensity map of the white light emission of (a). The $Tb_{0.6}Sc_{0.4}Ca_4O(BO_3)_3$ region had the brightest emission. There was no positive effect of Pr.

computer simulation of the method was verified in the optimization of light emitting properties in the ternary system of calcium oxyborates of Tb, Sc, and Pr. This method drastically speeds up the screening of ternary composition materials and can be extended to complicated multicomponent systems.

Acknowledgment. The authors thank Prof. K. Sasaki, Prof. Y. Mori, and Dr. Yoshimura of Osaka University for supplying the YCOB single crystals. We are also grateful to Prof. M. Ohtsu, Dr. T. Kawazoe, and Dr. K.-W. Kim of Tokyo Institute of Technology for providing us access to the PL measurement. This work was supported by the COMET (Combinatorial Materials Exploration and Technology) project.

Note Added after ASAP Posting

This paper was inadvertently posted before all corrections had been made. In the second paragraph of the Experimental Section, Al_2O_3(0001) and YCOB(100) notation was changed. The corrected paper was posted on November 17, 2003.

References and Notes

(1) Xiang, X.-D.; Sun, X.; Briceno, G.; Lou, Y.; Wang, K.-A.; Chang, H.; Wallace-Freedman, W. G.; Chen, S.-W.; Schultz, P. G. *Science* **1995**, *268*, 1738.
(2) Takeuchi, I.; van Dover, R. B.; Koinuma, H. *Combinatorial Materials Science. MRS Bull.* **2002**, 301.
(3) Matsumoto, Y.; Murakami, M.; Jin, Z.; Ohtomo, A.; Lippmaa, M.; Kawasaki, M.; Koinuma, H. *Jpn. J. Appl. Phys.* **1999**, *38*, L603.
(4) van Dover, R. B.; Schneemeyer, L. F.; Fleming, R. M. *Science* **1998**, *392*, 162.
(5) Fukumura, T.; Ohtani, M.; Kawasaki, M.; Okimoto, Y.; Kageyama, T.; Koida, T.; Hasegawa, T.; Tokura, Y.; Koinuma, H. *Appl. Phys. Lett.* **2000**, *77*, 3426.
(6) Matsumoto, Y.; Murakami, M.; Shono, T.; Hasegawa, T.; Fukumura, T.; Kawasaki, M.; Ahmet, P.; Chikyow, T.; Koshihara, S.; Koinuma, H. *Science* **2001**, *291*, 854.
(7) Takahashi, R.; Matsumoto, Y.; Koinuma, H.; Lippmma, M.; Kawasaki, M. *Appl. Surf. Sci.* **2002**, *197*−*198*, 532.
(8) Miller, N. C.; Shirn, G. A. *Appl. Phys. Lett.* **1967**, *10*, 86.
(9) Hanak, J. J. *J. Mater. Sci.* **1970**, *5*, 964.
(10) Koinuma, H.; Kawasaki, M.; Nagata, S.; Takeuchi, K.; Fueki, K. *Jpn. J. Appl. Phys.* **1988**, *27*, L376.
(11) Danielson, E.; Golden, J. H.; McFarland, E. W.; Reaves, C. M.; Weinberg, W. H.; Wu, X. D. *Nature* **1997**, *389*, 944.
(12) Chang, H.; Takeuchi, I.; Xiang, X.-D. *Appl. Phys. Lett.* **1999**, *74*, 1165.
(13) Hasegawa, K.; Ahmet, P.; Okazaki, N.; Hasegawa, T.; Fujimoto, K.; Watanabe, M.; Chikyow, T.; Koinuma, H. *Appl. Surf. Sci.*, in press.
(14) Iwai, M.; Kobayashi, T.; Furuya, H.; Mori, Y.; Sasaki, T. *Jpn. J. Appl. Phys.* **1997**, *36*, L276.
(15) Kim, T.-W.; Arai, N.; Matsumoto, Y.; Yoshimura, M.; Furuya, H.; Mori, Y.; Sasaki, T.; Koinuma, H. *J. Cryst. Growth* **2001**, *229*, 208.

CC030038I